Modes of Annular Variability in the Atmosphere and Eddy-Zonal Flow Interactions

Sarah Sparrow[1,2], Mike Blackburn[2] and Joanna Haigh[1]

[1]Space and Atmospheric Physics, Imperial College London, UK
[2]Department of Meteorology, University of Reading, UK

1. Background

Idealised model experiments (Haigh *et al.* 2005; Haigh and Blackburn 2006), have shown that changes to the stratospheric equilibrium temperature distribution lead to changes in the strength and position of the tropospheric jets and storm tracks, the extent of the Hadley cells and mean meridional circulation. Here we investigate how such shifts in the tropospheric jet can be understood by examining combined fluctuations of the first two modes of annular variability. Attention is paid to the evolution of the flow on different timescales as defined by empirical mode decomposition.

2. Model Experiments

Idealised experiments were performed using a simplified global circulation model (sGCM). The model uses the spectral dynamical core described by Hoskins and Simmons (1975) with a T42L15 resolution and a top level of 18 hPa. Temperature is relaxed towards the zonally symmetric equilibrium temperature distribution, T_e (latitude, sigma), of Held and Suarez (1994). The results presented use 10,000 days of simulation which are effectively doubled as results from each hemisphere are treated as independent realisations (possible because temporal correlations between two hemispheres are very low (~0.2)).

3. Variability of Zonal Mean Flow (EOFs)

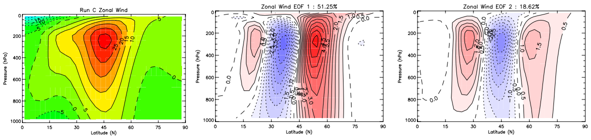

Figure 1: Time mean zonal wind, EOF1 and EOF2 calculated from zonal mean zonal wind anomalies (ms^{-1}). The variance explained by each is noted in the title.

The two principal modes of annular variability are shown in figure 1 as identified by a principal component analysis of the daily zonal mean zonal wind anomaly. Appropriate latitudinal and pressure weightings are applied to ensure that equal masses are afforded equal weight. The time mean jet is shown for comparison. EOF1 represents a latitudinal shift of the mean jet and EOF2 strengthening (weakening) and narrowing (broadening) of the jet.

4. Empirical Mode Decomposition

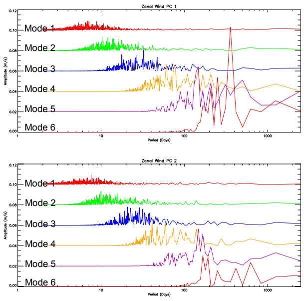

Figure 2: Fourier spectra for EMD modes for PC1 (top panel) and PC2 (bottom panel). Each mode has been offset by 0.02 ms^{-1} for clarity.

Empirical mode decomposition (EMD) is a technique for analysing different timescales in non-linear and non-stationary data (Huang et al. 1998). Performing this analysis on PC1 and PC2 produces modes that are similar to band-pass filtered data without having to specify specific band limits (figure 2).

For a given mode a similar frequency band is sampled for both PC1 and PC2. This enables examination of a combined mode in a PC1/PC2 phase space.

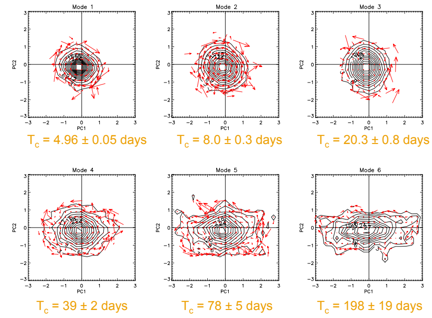

Figure 3: PC phase space for each EMD mode. Black contours indicate the density of points. Vectors show the mean trajectory at each location.

Figure 3 shows phase space distributions for EMD modes.

Modes 1-2 (high frequency) have clockwise evolution and a circular distribution (equal contributions from PC1 and PC2).

Mode 3 shows no clear circulation and is a transition between high and low frequencies.

Modes ≥ 4 (low frequency) have anticlockwise evolution and the distribution is elongated along PC1.

Circulation timescales (Tc) increase approximately exponentially with each mode.

5. Transformed Eulerian Mean (TEM) Momentum Budget - 1

$$\boxed{\frac{d[u]}{dt}} = \boxed{\frac{1}{a\cos\phi}\nabla\cdot\mathbf{F}} + \boxed{-\left\{f[v^*] + \frac{[v^*]}{a\cos\phi}\frac{\partial}{\partial\phi}([u]\cos\phi) + [w^*]\frac{\partial[u]}{\partial p}\right\}} + \boxed{[F_\lambda]}$$

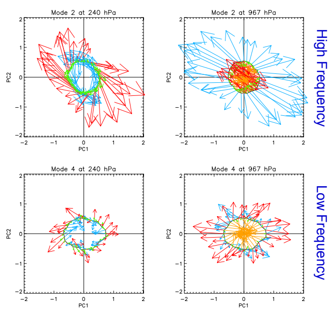

Figure 5: Sector composite average trajectory (black line) for modes 2 and 4 at 240 and 967 hPa. Vector budget show the projection of TEM terms into PC1/PC2 phase space. EP Flux divergence (red); residual circulation (blue); surface stress (orange) and wind tendency (green).

In the TEM momentum budget (formula above) the zonal wind acceleration (green) consists of an eddy term (red), a residual circulation term (blue) and the surface stress (orange).

Figure 4 summarises the effect on the current zonal wind anomalies of radial and tangential movements in phase space.

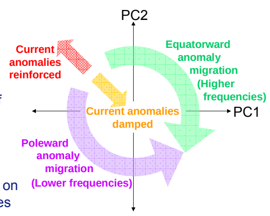

Figure 4: Interpretation of radial and tangential movements in phase space.

Figure 5 shows the projection of TEM momentum budget terms into phase space.

For mode 2 (high frequency) at upper levels the eddies (red) strongly drive the equatorward phase space evolution but are opposed by the residual circulation term (blue). At lower levels the eddy term is out of phase with the wind anomalies and is a lagged response to previous wind anomalies.

For mode 4 (low frequency) at upper levels the eddies drive the poleward anomaly migration. This is strongly but not completely balanced by the residual circulation term. At lower levels the eddies point radially outwards and reinforce the current wind anomalies. They are balanced by the surface stress (orange) which damps current anomalies. Phase space circulation is governed by the residual circulation at lower levels.

6. Transformed Eulerian Mean Momentum Budget - 2

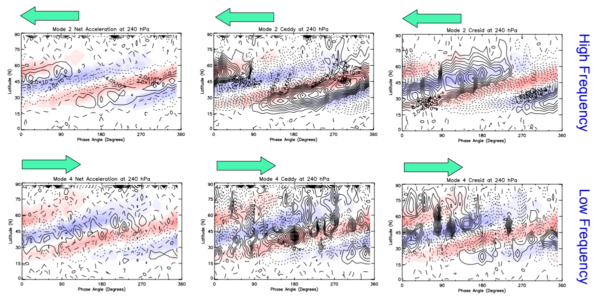

Figure 6: Latitude-phase angle sections for mode 2 and 4 at 240 hPa for TEM momentum budget terms (contours; solid positive values, dashed negative values). Colours represent zonal mean zonal wind anomalies (red positive values and blue negative values). Green arrows indicate the propagation direction for each plot.

Figure 6 shows latitude-phase angle sections for TEM momentum budget terms. At both high and low frequencies the net acceleration from the momentum budget (left column, contours) is in quadrature with the zonal wind anomalies (colours) at all phase angles. In the upper troposphere the net acceleration is dominated by the eddy term (middle column, contours) which is strongly, but not completely balanced by the residual circulation term (right column, contours).

7. Mechanism

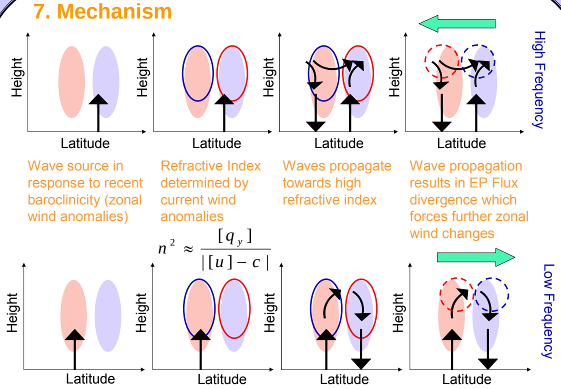

Figure 7: Schematic sections for high and low frequency modes. Colour filled ovals represent zonal wind anomalies and arrows represent wave propagation. In the middle two diagrams the open circles represent refractive index anomalies and, in the right hand panel, the EP flux divergence forcing anomalies (dashed). The green arrows represent the resulting anomaly propagation direction.

8. Mechanism: Data from single composite

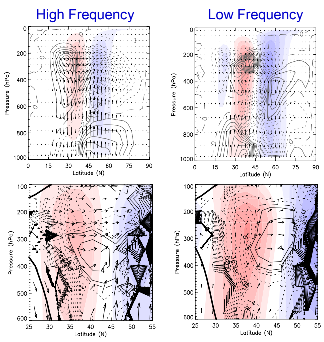

Wave source responds to recent past. Wave propagation in response current zonal wind anomalies and results in upper level EP Flux divergence which forces further zonal wind changes.

Refractive Index anomalies determined by wind anomalies.

$$n^2 \approx \frac{[q_y]}{|[u]-c|}$$

Waves propagate towards high refractive index.

Figure 8: Latitude-height sections for an example composite (-ve PC1) from a high and low frequency mode. The upper row shows zonal wind anomalies (colours), EP flux divergence forcing (contours) and EP flux vector anomalies (arrows). The bottom row shows zonal wind anomalies (colours), refractive index anomalies (contours) and EP flux vector anomalies (arrows) . Solid contours and red shading represent positive values, dotted contours and blue shading represents negative values.

9. Conclusions

At high frequencies, zonal mean jet anomalies propagate equatorwards.

At low frequencies, zonal mean jet anomalies propagate polewards.

The jet migration for all timescales is driven by the eddies at upper levels and conveyed to lower levels by the residual circulation. The wave source responds to the past baroclinicity of the flow, but propagation occurs through the current wind anomalies. At higher frequencies the flow is so strongly eddy driven that the current zonal wind anomalies have changed sufficiently to be ~180° out of phase with the wave source. At lower frequencies the wave source is almost in phase with the current wind anomalies.

On all timescales the waves propagate towards high refractive index which in turn is dominated by the current wind anomalies. The resulting wave propagation gives rise to EP flux divergence anomalies, which at upper levels force the observed latitudinal shift of the jet either equatorwards (high frequencies) or polewards (low frequencies).

Acknowledgements

This work is supported by the UK Natural Environment Research Council through the SOLCLI Consortium Grant.

References

Haigh, J. D., M. Blackburn and R. Day, 2005: The response of tropospheric circulation to perturbations in lower-stratospheric temperature. *J. Clim.*, **18** (17), 3672-3685.

Haigh, J. D., and M. Blackburn, 2006: Solar influences on dynamical coupling between the stratosphere and troposphere. *Space Science Reviews*, **125** (1-4),331-344.

Held, I. M. and M. J. Suarez, 1994: A proposal for the intercomparison of the dynamical cores of atmospheric general circulation models. *Bull. Amer. Meteor. Soc.*, **75**, 1825-1830.

Hoskins, B. J. and A. J. Simmons, 1975: A multi-layer spectral model and the semi-implicit method. *Q. J. R. Meteorol. Soc.*, **101**, 637-655.

Huang, N. E. et al., 1998: The empirical mode decomposition and the Hilbert spectrum for non linear and non-stationary time series analysis. *Proc. R. Soc. Lond. A*, **454**, 903-995.